The colours of satellite galaxies in groups and clusters

A. S. Font,[1]★ R. G. Bower,[1] I. G. McCarthy,[1] A. J. Benson,[2] C. S. Frenk,[1] J. C. Helly,[1] C. G. Lacey,[1] C. M. Baugh[1] and S. Cole[1]

[1]*Department of Physics, University of Durham, South Road, Durham DH1 3LE*
[2]*Theoretical Astrophysics, Caltech, MC130-33, 1200 E. California Blvd., Pasadena CA 91125, USA*

ABSTRACT

Current models of galaxy formation predict satellite galaxies in groups and clusters that are redder than observed. We investigate the effect on the colours of satellite galaxies produced by the ram-pressure stripping of their hot-gaseous atmospheres as the satellites orbit within their parent halo. We incorporate a model of the stripping process based on detailed hydrodynamic simulations within the Durham semi-analytic model of galaxy formation. The simulations show that the environment in groups and clusters is less aggressive than previously assumed. The main uncertainty in the model is the treatment of gas expelled by supernovae. With reasonable assumptions for the stripping of this material, we find that satellite galaxies are able to retain a significant fraction of their hot gas for several Gyr, thereby replenishing their reservoirs of cold, star-forming gas and remaining blue for a relatively long period of time. A bimodal distribution of galaxy colours, similar to that observed in Sloan Digital Sky Survey data, is established and the colours of the satellite galaxies are in good agreement with the data. In addition, our model naturally accounts for the observed dependence of satellite colours on environment, from small groups to high-mass clusters.

Key words: galaxies: clusters: general – galaxies: evolution – galaxies: fundamental parameters – galaxies: luminosity function, mass function.

1 INTRODUCTION

Recent multiwavelength imaging with the Sloan Digital Sky Survey (SDSS; York et al. 2000) has convincingly demonstrated that the colour–magnitude distribution of galaxies is bimodal (Strateva et al. 2001; Hogg et al. 2002; Blanton et al. 2003; Baldry et al. 2006). Other galaxy properties, such as the star-formation rates, disc-to-bulge ratios, concentrations, stellar surface mass densities and gas-mass fractions also show bimodal distributions (Kauffmann et al. 2003; Balogh et al. 2004; Brinchmann et al. 2004; Hogg et al. 2004; Kannappan 2004). Elucidating the origin of these distributions requires understanding whether they arise in situ or whether they are environmentally driven (i.e. the 'nature' or 'nurture' dichotomy).

While they are not the only means by which theorists attempt to tackle the problem of galaxy formation, at present semi-analytic models offer the best hope for understanding the origin of the bimodality. The level of sophistication of these models has grown rapidly in recent years and so too has their ability to match a wide variety of observational data [Kauffmann, White & Guiderdoni 1993; Lacey et al. 1993; Cole et al. 1994; Kauffmann et al. 1999; Somerville & Primack 1999; Cole et al. 2000; Benson et al. 2002,

2003; Baugh et al. 2005; Bower et al. 2006 (hereafter B06); Croton et al. 2006]. The recent addition of feedback from active galactic nuclei (AGN) in the semi-analytic models (e.g. Granato et al. 2004; B06; Cattaneo et al. 2006; Croton et al. 2006; Kang, Jing & Silk 2006; Menci et al. 2006) has provided an explanation for three well-known, yet puzzling observational results: (i) the steep cutoff at the bright end of the galaxy luminosity function, (ii) the fact that most massive galaxies today tend to be dominated by old, red stellar populations and (iii) the absence of classical cooling flows in the centres of massive X-ray clusters. In addition, some of these models (e.g. that of B06, which we adopt as the baseline model in this paper) are also able to reproduce the evolution of the *K*-band luminosity and the galaxy stellar mass functions out to high redshift (see Baugh 2006, and references therein for a more in-depth discussion of the successes and limitations of semi-analytic models).

In terms of galaxy colours, semi-analytic models with AGN feedback are able to produce a clear bimodal separation of colours at high luminosities, match the slope of the red and blue sequences and explain the absence of massive blue galaxies. However, it has recently become clear that these models are unable to match the relative numbers of faint satellite galaxies on the red and blue sequences. Specifically, Weinmann et al. (2006b) and Baldry et al. (2006) have shown that the faint satellite galaxies in groups and clusters modelled semi-analytically are on average too red in comparison to satellite galaxies of similar luminosity in the SDSS

★E-mail: andreea.font@durham.ac.uk

sample. Using DEEP2 data, Coil et al. (2008) have shown that a similar problem may exist at higher redshifts ($z \sim 0.7$–0.9), where the semi-analytic models predict a stronger clustering of red galaxies than is observed. These results indicate that one or more physical processes (either internal or environmentally driven) that affect the ability of the galaxies to form stars are not yet accurately accounted for in the models.

In the present study, we concentrate on the effect of environmental processes on the colours of galaxies, particularly on the role that the ram-pressure stripping of the hot gas from galaxy haloes plays. At present, the semi-analytic models outlined above treat the stripping of the hot gas from the haloes of galaxies in a crude fashion, by assuming that the gaseous halo is completely and instantaneously stripped as the system crosses the virial radius of the (more massive) parent system and becomes a satellite. A direct consequence of this stripping is that the only fuel that is available for star formation once the galaxy becomes a satellite is that which resided in a cold disc when the galaxy first fell into the halo. As a result, the satellite galaxy experiences a sharp decline in its star-formation rate and its stellar population becomes red over time. This process of cutting off the supply of hot gas that would otherwise cool and replenish the reservoir of cold, star-forming gas, is sometimes referred to as 'strangulation' or 'starvation' (Larson, Tinsley & Caldwell 1980; Balogh, Navarro & Morris 2000). It is clear, however, that the maximally efficient stripping assumed by most current semi-analytic models is not realistic, especially in cases where the mass of the satellite is comparable to that of the parent system (Wang et al. 2007).

In a very recent study, Kang & van den Bosch (2008) investigate the effect of modelling the stripping of satellites by an exponential decay. They adopt a stripping factor that is independent of the properties and orbit of the parent and satellite haloes and vary this to achieve the best match to the observations. However, although this empirical approach is a step forward, one expects the efficiency of the stripping to depend on the orbit of the satellite and on the structural properties of both the satellite and parent systems. In contrast, the model we present here aims to implement a physically motivated description for the stripping effect, taking into account the relevant properties of the system.

Recently, McCarthy et al. (2008) carried out a large suite of high-resolution hydrodynamic simulations of the stripping of the hot-gaseous haloes of galaxies and presented a simple, physically motivated model that describes the simulation results remarkably well. These authors concluded that, typically, galaxies are able to retain a significant fraction of their hot haloes for long periods of time following virial crossing. The results of these simulations are in qualitative agreement with a recent *Chandra* X-ray survey of massive satellite galaxies in hot clusters by Sun et al (2007), who found that most massive satellites do indeed have detectable hot haloes (see also Jeltema, Binder & Mulchaey 2008). The implication of these results is that the stripping of the hot-gaseous haloes is much less efficient than previously assumed. Consequently, some replenishment of the cold star-forming reservoir (via cooling of the hot halo) in the satellite galaxies is expected to take place, this prolonging star formation and resulting in bluer satellite galaxies.

In the present study, we incorporate the prescription for ram-pressure stripping of hot haloes of McCarthy et al. (2008) in the Durham semi-analytic code for galaxy formation, GALFORM, and show that this improvement in environmental physics brings the colours of satellite galaxies into much better agreement with the observational data.

The layout of the paper is as follows. In Section 2, we present the details of the implementation of the new ram-pressure model in GALFORM. In Section 3, we present results for the fraction of blue galaxies in the new model (Section 3.1), discuss the environmental signatures in the colours of galaxies (Section 3.2) and present predictions for the red and blue luminosity functions at redshift $z = 0.1$ for galaxies of different type (Section 3.3). In Section 4, we summarize and discuss our findings.

2 A SEMI-ANALYTIC MODEL OF GALAXY FORMATION WITH RAM-PRESSURE STRIPPING OF HOT-GASEOUS HALOES

2.1 The B06 version of GALFORM

Apart from the minor changes described below, we use the version of GALFORM semi-analytic code described in B06. This version of GALFORM makes use of halo merger histories extracted from the *Millennium Simulation* with the techniques of Helly et al. (2003) (see also Harker et al. 2006). The *Millennium Simulation* (Springel et al. 2005) was carried out by the Virgo Consortium and it is one of the largest simulations of the growth of structure in the Λ cold dark matter cosmology to date, containing approximately 10 billion dark matter particles in a cubic volume of $(500\,h^{-1}\,\mathrm{Mpc})^3$ with a particle mass of $8.6 \times 10^8\,\mathrm{M_\odot}\,h^{-1}$. Throughout the paper we adopt the same cosmological model assumed in the Millennium simulation (and in the B06 model) and quote our results in terms of the Hubble variable $h = H_0/100\,\mathrm{km^1\,Mpc^{-1}}$.

In terms of baryonic physics, the version of GALFORM developed by B06 has the same basic structure as in Cole et al. (2000), but with the addition of an improved treatment of gas cooling and a new scheme for AGN feedback. In the present study, most of the basic parameters of the code (including, e.g. the efficiencies of supernovae and AGN feedback and the time-scales for star formation and dynamical friction) are the same as those adopted in B06. However, in order to achieve better agreement with the zero-point colours of the observed red and blue sequences, we increase the value of the yield to $p = 0.04$, which is a factor of two higher than the 'standard' solar value adopted by B06. With this change, the $^{0.1}(g - r)$ colours are redder by 0.1 mag compared with those in the B06 model (for galaxies on the red sequence). It also improves the metallicity of the intracluster medium (ICM): whereas in the standard B06 model the metallicity of the ICM was too low, $Z_{\mathrm{ICM}} \simeq 0.15\,Z_\odot$, in the model with double the yields $Z_{\mathrm{ICM}} \simeq 0.3\,Z_\odot$ (Bower, McCarthy & Benson 2008), a value which is in better agreement with the X-ray measurements (e.g. Baumgartner et al. 2005). We note that large yields such as these have been used in semi-analytical models in the past in order to get better agreement between the model predictions for galaxy colours and the observations (see Kauffmann & Charlot 1998; de Lucia, Kauffmann & White 2004; but see also the discussion of Cole et al. 2000 about increasing yields and consistency with stellar evolution models).

One further minor change from the version of B06 concerns the division between haloes in the rapid cooling and hydrostatic regimes. B06 adopted a sharp transition between these two regimes. In particular, the BO6 model assumes that radio-mode feedback is only effective in hydrostatic haloes with

$$t_{\mathrm{cool}}(r_{\mathrm{cool}}) > \alpha_{\mathrm{cool}}^{-1} t_{\mathrm{ff}}(r_{\mathrm{cool}}), \tag{1}$$

where t_{cool} and r_{cool} are the cooling time and radius, t_{ff} is the free-fall time (as defined by Cole et al. 2000) and α_{cool} is an adjustable parameter (set in this model to 0.7) that rescales the freefall time of

the halo and has the effect of controlling the position of the break in the luminosity function.[1] If the above condition is satisfied, it is then determined whether or not the central AGN is able to inject sufficient power to offset the energy being radiated away in the cooling flow and, if the available AGN power is greater than the cooling luminosity, the cooling flow is assumed to be completely quenched.

This strict dichotomy in halo properties has the undesirable effect that small changes in, for example, the gas-mass fraction of haloes near the transition can greatly affect the star-formation rate in their central galaxy. This leads to a small population of rapidly forming galaxies at the bright end of the blue sequence. In the present paper, we have refined the criterion to make the transition more gradual. To do this, we reduce the cooling rate in haloes for which the cooling radius and effective freefall radius [$r_{cool}(t)$ and $r_{ff,eff}(t) \equiv r_{ff}(\alpha_{cool}t)$] are close to each other. Specifically, if

$$|r_{cool} - r_{ff,eff}| \leq 0.5\epsilon_{cool}^{-1}r_{cool}, \qquad (2)$$

the net cooling rate is reduced:

$$\dot{m}_{cool,eff} = \dot{m}_{cool}\left[0.5 + \epsilon_{cool}(1 - r_{ff}/r_{cool})\right], \qquad (3)$$

where $\dot{m}_{cool}$ is the cooling rate in the absence of AGN feedback. This function leaves the cooling rate unchanged if the inequality above is not satisfied. For large values of ϵ_{cool}, the inequality applies for only a narrow range of ($r_{cool} - r_{ff,eff}$), and the behaviour of the B06 model is maintained. Here, we adopt $\epsilon_{cool} = 10$, so that the transition is still quite sharp, and the luminosity function is little affected. The effect on the colours of galaxies at the bright tip of the blue sequence is, however, noticeable: by suppressing gas cooling in these objects, the tip of the blue sequence becomes redder, tending to curl up towards the red sequence. This provides a slightly better match to observational data in this part of the colour–magnitude diagram (see Section 3.1).

With these basic parameters, we run a model with a complete and instantaneous ram-pressure stripping of the hot-gaseous haloes of satellites (the 'default' model) and a model where the ram-pressure stripping of the hot haloes of satellites is calculated using the prescription of McCarthy et al. (2008) (henceforth called the 'hot ram-pressure model').

2.2 Implementation of ram-pressure stripping

Below we give a brief description of the McCarthy et al. (2008) ram-pressure stripping model and how it is incorporated into GALFORM. The McCarthy et al. model is analogous to the original formulation of Gunn & Gott (1972) for the stripping of a face-on cold disc, except that it applies to a spherical distribution of hot gas. Specifically, the hot-gaseous halo of the satellite will be stripped if the ram pressure (P_{ram}) exceeds the satellite's gravitational restoring force per unit area (P_{grav}):

$$P_{ram} \equiv \rho_{gas,p}v_{sat}^2 > P_{grav} \equiv \alpha_{rp}\frac{GM_{tot,sat}(r)\rho_{gas,sat}(r)}{r}, \qquad (4)$$

where $\rho_{gas,p}$ is the gas density of the parent halo, v_{sat} is the velocity of the satellite with respect to this medium, $M_{tot,sat}(r)$ is the total mass of the satellite within radius r and $\rho_{gas,sat}(r)$ is the density of the satellite's hot halo at this radius. The coefficient α_{rp} is a geometric constant of order unity; McCarthy et al. find that $\alpha_{rp} \approx 2$ gives the best fit to their hydrodynamic simulations. Note that

equation (4) has not introduced any new free parameters into the GALFORM semi-analytical model, as α_{rp} has been tuned to match the results of hydrodynamic simulations.

The satellite-centric radius where $P_{ram} = P_{grav}$ is referred to as the stripping radius and McCarthy et al. assume that within this radius the satellite's gaseous halo remains intact while all gas exterior to this radius is stripped on approximately a sound crossing time. This physically simple model has been shown to match the results of their high-resolution hydrodynamic simulations[2] remarkably well for a wide range of orbits, mass ratios, and structural properties.

In our implementation of the hot ram-pressure model, we fix the stripping radius by setting the ram pressure to its maximum value, which occurs at the pericentre of the satellite's orbit, and the gas is stripped at the instant it crosses the virial radius. We adopt this simplification as, by default, GALFORM does not track the full orbital evolution of the satellite galaxies (but see Benson et al. 2003).[3] In reality, the physical size of the stripping radius is a function of time, as the magnitude of the ram pressure varies along a non-circular orbit. By setting the ram pressure to its maximum value, we overestimate the amount of stripping that occurs between the time when the satellite crosses the virial radius of the parent halo and when it reaches pericentre for the first time. However, for typical orbits this is not unreasonable, since this time-scale is generally a small fraction of the total amount of time that the satellite spends in orbit about the parent halo. In addition, since the full orbital evolution of the satellites is not followed, we neglect the effects of tidal heating and tidal stripping of the satellite system. In terms of the removal of hot halo gas, however, ram-pressure stripping is a more efficient mechanism than tidal stripping for the vast majority of satellites (i.e. the stripping radius is typically smaller than the satellite's tidal radius; see McCarthy et al. 2008).

The pericentres and the velocities at pericentre (both of which are required to compute the maximum ram pressure along the orbit) of the satellites are calculated by assuming the satellites have the same 2D joint radial (v_r) and tangential (v_θ) velocity distribution of infalling substructure as measured by Benson (2005) from a large suite of Virgo Consortium cosmological simulations. Benson (2005) finds that the following functional form describes the 2D distribution well:

$$f(v_r, v_\theta) = a_1 v_\theta \exp\left[-a_2(v_\theta - a_9)^2 - b_1(v_\theta)(v_r - b_2(v_\theta))^2\right], \quad (5)$$

where $a_1, a_2, a_9, b_1(v_\theta)$ and $b_2(v_\theta)$ are coefficients and functions tabulated in Benson (2005). We assume that this distribution is independent of halo mass and redshift. For each satellite, we randomly sample this distribution, extracting a radial and tangential velocity pair which, in turn, allows us to calculate the energy and angular momentum (per unit mass) of the orbit. We compute the pericentre radius and velocity of the satellite at pericentre by assuming that the orbital energy and angular momentum are conserved and by treating the satellite as a point mass orbiting within a Navarro–Frenk–White

---

[1] Equation (2) of B06 is incorrect; α_{cool} should be replaced by α_{cool}^{-1}.

---

[2] This includes both Lagrangian smooth particle hydrodynamic simulations with the GADGET-2 code (Springel 2005) and Eulerian adaptive mesh refinement simulations with the FLASH code (Fryxell et al. 2000).

[3] The Millennium simulation provides full dynamical information for subhaloes until they are tidally disrupted. In view of the limited reaolution of the simulation, however, we choose to calculate the merging timescale of subhaloes using the standard Chandrasekhar (1943) formula rather than following the subhalo orbits explicitly, as explained in BO6. Since we are interested mainly in the broad statistical distribution of galaxy colours, our results should not be affected by the loss of information about individual orbits.

(NFW) (Navarro, Frenk & White 1996, 1997) potential with the same total mass and concentration as the parent halo (see, e.g. Binney & Tremaine 1987). By assuming that the orbital energy and angular momentum are conserved, we are ignoring the dynamical friction force acting on the satellites. However, in cases where the dynamical friction force is strong, the satellite will quickly sink to the centre of the parent halo and, in any case, this process is important for the most massive satellites which are less affected by ram-pressure stripping.

By default, the version of GALFORM presented in B06 assumes that the gas density profiles of the hot haloes of all systems (including satellite systems) follow a β-model (Cavaliere & Fusco-Femiano 1976, 1978), with $\beta = 2/3$ (which provides a reasonable match to the X-ray surface brightness profiles of massive groups and clusters; Jones & Forman 1984), a fixed core radius $r_c = 0.1R_{vir}$, and a normalization ρ_0 that is set to yield the correct mass of hot gas within the virial radius. We adopt the same distribution in the present study. We note, however, that we have also experimented with NFW density profiles for the hot gas (for both the satellite and parent systems), and find that the resulting fraction of satellite galaxies that are blue is quite similar to the case of the β-model. This is likely to stem from the fact that, typically, the hot gas is only stripped down to intermediate radii, where the β-model and the NFW profile are similar.

In addition to a hot tenuous atmosphere, each halo has a reservoir of cold gas that developed from the cooling of the hot atmosphere and which can potentially form stars. As stars are formed, some of this cold gas is re-heated by feedback from, for example, supernovae winds. Prior to stripping, the re-heated gas is assumed to follow the same spatial and thermodynamic distribution as the hot gas in the halo (as in B06). We therefore treat the initial stripping of re-heated gas in the same fashion as the hot gas, and transfer the same fraction (as computed with the ram-pressure stripping algorithm described above) from the re-heated gas of the satellite to the re-heated gas reservoir of the parent halo. We record the total mass stripped from the halo as M_{strip} and the fraction of the hot halo that is stripped as f_{strip}. Although this procedure is simple, it is worth noting that in reality the spatial and thermodynamic properties of the re-heated gas could be quite complicated (e.g. multiphase) and that it need not be distributed in the same way as the hot-gas phase. It would be worth revisiting this issue once a better treatment of the re-heated gas is incorporated into the semi-analytic model (Benson et al., in preparation).

The cooling rate of the remaining, unstripped gas is calculated by cooling only the gas within the stripping radius and assuming that stripping does not alter the mean density of gas within this radius. We implement this by giving the satellite a nominal hot-gas mass $M'_{hot} = M_{hot} + M_{strip}$ (where M_{hot} is the true hot-gas content of the halo) and applying the same cooling algorithm as that used for central galaxies (except limiting the maximum cooling radius to r_{strip} rather than R_{vir}). This step ensures self-consistency in the treatment of the gas cooling between stripped and unstripped galaxies, and therefore that the colours of satellites are predicted correctly.

So far, we have only been considering the stripping of gas which was in the hot or re-heated phases at the time the satellite halo reached pericentre in the parent halo for the first time. However, as long as star formation continues in the satellite galaxy, supernova feedback will continue to re-heat gas and eject it from the satellite galaxy. The colours of satellite galaxies turn out to be sensitive to how much of this 'secondary' re-heated gas is stripped. The numerical simulations of McCarthy et al. (2008) do not provide any direct information about the stripping of this re-heated gas, since

they only treat the stripping of the initial hot halo. One can imagine several possible scenarios for the fate of the re-heated gas: we adopt a picture in which the re-heated gas is ballistically ejected as relatively cold material that subsequently mixes or evaporates to become part of the hot halo. In isolated galaxies, the re-heated gas is put back with the same radial distribution as for the original hot-gas halo. In satellite galaxies, we can consider two extreme cases for the treatment of the secondary re-heated gas. Continuing to apply the initial stripping criterion to the satellite galaxy as it orbits suggests that the re-heated gas should be stripped by the same factor f_{strip} as it is ejected from the galaxy. However, applying this at every timestep is too extreme: most of the re-heating occurs during the outer part of the galaxy's orbit where the ram-pressure force is small. It might therefore be more appropriate to consider a second case where little of this re-heated gas is stripped by ram-pressure effects. Further numerical simulations are required to elucidate which of these scenarios is physically more realistic and to determine a suitable parameterization of the time averaged stripping rate. At this point, the second (minimal stripping) case seems more appropriate since the typical orbital time-scale exceeds several Gyr, and is comparable to the time-scale for the mass-growth of the parent halo (see below).

To allow for these uncertainties, we adopt a partially empirical approach, and model the time-dependence of the hot-gas mass in the satellite halo after its first pericentre passage as:

$$\dot{M}_{hot} = (1 - \epsilon_{strip} f_{strip}) \frac{M_{reheat}}{\tau_{reheat}} - \dot{M}_{cool}, \qquad (6)$$

Here, M_{hot} is the mass of hot gas available for cooling and $\dot{M}_{cool}$ is the rate at which it cools. M_{reheat} is the mass of gas which has been re-heated by supernovae but not yet returned to the hot phase. In the absence of ram-pressure stripping, this re-heated gas is assumed to return to the hot phase on a time-scale $\tau_{reheat} = t_{dyn}/\alpha_{reheat}$, as in B06, where the value $\alpha_{reheat} = 1.26$ was chosen to match the observed galaxy luminosity function. The effect of ram-pressure stripping is described by the term $\epsilon_{strip} f_{strip}$, where f_{strip} is the stripping factor already calculated for the initial pericentre using equation (4), and ϵ_{strip} is a new parameter (representing the time averaged stripping rate after the initial pericentre) which we adjust to fit the observations. The first (maximal) stripping case corresponds to $\epsilon_{strip} = 1$ if the orbital time-scale is much shorter than the re-heating time-scale, and the second case (minimal stripping) to $\epsilon_{strip} = 0$. The gas which is stripped from each satellite is added to the hot-gas component of the parent halo.

We find that if we take $\epsilon_{strip} = 1$, then the colour distribution of satellite galaxies looks very similar to the default model in which there is complete stripping of the initial hot gas and of the re-heated gas, with all satellites lying on the red sequence. For $0.2 \lesssim \epsilon_{strip} < 1$, the satellite colour distribution looks similar to the case $\epsilon_{strip} = 1$. For $\epsilon_{strip} \lesssim 0.2$, a blue sequence appears for the satellites, which results in better agreement with the observed colour–magnitude distribution. Values in the range $0 \leq \epsilon_{strip} \lesssim 0.2$ result in similar colour–magnitude distributions. For this paper, we adopt the value $\epsilon_{strip} = 0.1$.

The stripping of satellites is also affected by the growth of the halo in which the satellite is orbiting. If we did not allow for the effect of halo growth, a small satellite accreted at high redshift would not feel the increasing ram-pressure effect as the parent halo grows in mass, perhaps becoming a galaxy cluster by the present day. In order to take this effect into account, we assign the satellite galaxy new orbital parameters and derive a new stripping factor every time the halo doubles in mass compared to the initial stripping event.
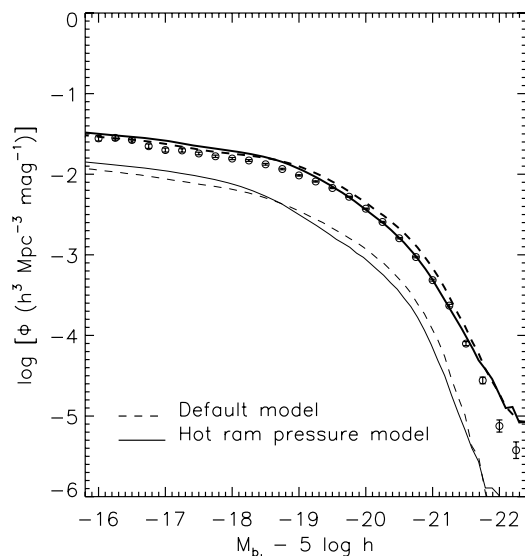
Figure 1. Comparison of the predicted galaxy luminosity functions of the default model with the hot ram-pressure stripping model at redshift $z = 0$. The data points represent observations from the 2dF Galaxy Redshift Survey (Norberg et al. 2002). Magnitudes are b_J (Vega) in both the models and the observations. Models use volume limited samples and the smallest resolved haloes have luminosities $\simeq 0.03\, L_*$ (equivalent to $M_{b_J} - 5\log h = -15.7$). Thick lines correspond to all galaxies and thin lines to satellite galaxies only.

If this factor exceeds that applied previously, additional hot and re-heated material is removed from the galaxy. This process tends additionally to suppress on-going star formation in the satellites of massive haloes.

An additional physical effect that may be relevant but that is not accounted for in our model is that the (ram + thermal) pressure force exerted on the hot halo of the satellite could, in turn, raise the pressure force exerted on the cold gas and potentially stimulate additional star formation (Bekki & Couch 2003). This would tend to result in bluer colours for the satellite galaxies. The magnitude of this effect is presently unclear, however, and needs to be quantified either observationally or with the aid of hydrodynamic simulations that accurately include the effects of cooling, star formation and feedback.

3 RESULTS

Since it is plausible that including a better treatment of the ram-pressure stripping may have a fairly significant impact on the observable properties of the galaxies, we first check if the predicted galaxy luminosity function is significantly altered.

In Fig. 1, we compare the predicted galaxy luminosity function for the default[4] and hot ram-pressure stripping models at redshift $z = 0$. The figure shows that our improved treatment of the ram pressure does not significantly alter the luminosity function. This is primarily because ram-pressure stripping preferentially affects satellite galaxies, whereas the total luminosity function (satellites + centrals) is dominated by central galaxies (see Section 3.3). In fact, even the luminosity function of satellite galaxies alone is only affected by a small amount (see thin lines in Fig. 1), however, as we

show below, the distribution of satellite colours at fixed luminosity is significantly altered.

3.1 The blue fraction of galaxies

Fig. 2 shows the predicted colour–magnitude diagram (CMD) of present-day galaxies for the default model (upper panels) and for the hot ram-pressure stripping model (lower panels). The three panels in each row, from left- to right-hand side, represent the CMDs of all galaxies, satellites only, and central galaxies only. For a more convenient comparison with the SDSS data, the model predictions are output at redshift $z = 0.1$ (which corresponds approximately to the median redshift of the SDSS sample) and the filters chosen for analysis are $^{0.1}g$ and $^{0.1}r$ in the AB system.

Fig. 2 shows, as expected, that changing the treatment of ram-pressure stripping primarily affects the colours of satellite galaxies. In particular, the distribution of $^{0.1}(g - r)$ colours at a fixed magnitude is broader for the hot ram-pressure stripping model and a larger fraction of the satellites now have bluer colours. The physical reason for this behaviour is simply that the retention of some of the hot gas in the halo of the satellite allows for the replenishment of the cold gas reservoir which, in turn, prolongs star formation in the satellite after its accretion on to the parent halo. Although the satellite galaxies eventually stop forming new stars as they consume their gas reservoir, this process is much more protracted in the hot ram-pressure model. As a result, the satellites cover a wider range of colours, filling in the region between the two main colour sequences. The red sequence is also much less pronounced in the new model.

To quantify this change in the colours, we classify galaxies as being either 'blue' or 'red' by adopting the colour cut proposed by Weinmann et al. (2006a) for galaxies in the SDSS that is
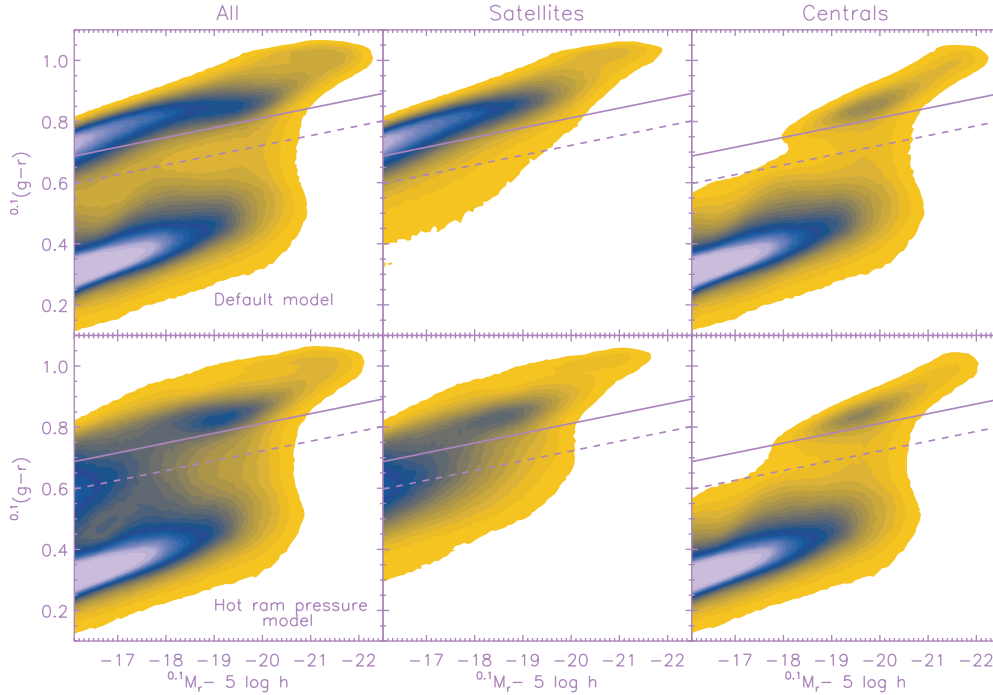
$$^{0.1}(g - r) = 0.7 - 0.032 \left(^{0.1}M_r - 5\log h + 16.5\right). \qquad (7)$$

This cut, which is represented in the panels of Fig. 2 by solid lines, isolates reasonably well the red and the blue sequences in both the default and hot ram-pressure models (see the top-left and bottom-left panels). This is similar to what is observed in the colour–magnitude diagram of SDSS galaxies (see fig. 1 of Weinmann et al. 2006a; also fig. 1 of Weinmann et al. 2006b). For the SDSS data, the cut adopted by Weinmann et al. tends to isolate the red sequence at its base defined at the high luminosity end (as opposed to following the minimum between the red and blue sequences). This effect is well reproduced by the solid line in Fig. 2.

We note, however, that adopting exactly the same colour cut in our models as in the observations is not necessarily the best choice. A drawback of using the Weinmann et al. colour cut to define blue and red fractions is that the results are quite sensitive to the precise position of the red sequence. For this reason, we also employ a second cut (indicated by the dashed line in Fig. 2), which intersects the model's bimodal contours roughly at their minimum. In the following, we will use by default the Weinmann et al. (2006a) cut and, for illustrative purposes, show also results with the alternative cut.

The left-hand and middle panels of Fig. 3 show, for the default and hot ram-pressure models respectively, the fraction of blue galaxies per $^{0.1}M_r$ magnitude for satellites (filled red circles), centrals (filled blue squares) and all types (filled green triangles) using the Weinmann et al. (2006a) cut. Also, shown is the fraction of blue satellites (open red circles) using the alternative colour cut.

Fig. 3 shows that the fraction of satellites that are blue in the hot ram-pressure model is about twice as high as in the default model.

---

[4] Our default model luminosity function is essentially the same as that of B06, even after the minor changes outlined in Section 2.2.

Figure 2. Colour–magnitude diagram (CMD) of $z = 0.1$ galaxies in the default model (upper panels) and in the hot ram-pressure stripping model (lower panels). The three panels in each row, from left- to right-hand side, represent the CMDs of all galaxies, satellites and central galaxies, respectively. Magnitudes are SDSS (AB system) $^{0.1}g$ and $^{0.1}r$ at redshift $z = 0.1$. The contours are spaced linearly in galaxy number density, starting from 500 per $(500\,h^{-1}\,\mathrm{Mpc})^3$ and increasing in levels of 500 per $(500\,h^{-1}\,\mathrm{Mpc})^3$. The solid line represents the colour cut adopted by Weinmann et al. (2006a) in order to separate blue and red galaxies in the SDSS. The dashed line represents an alternative colour cut (see text).
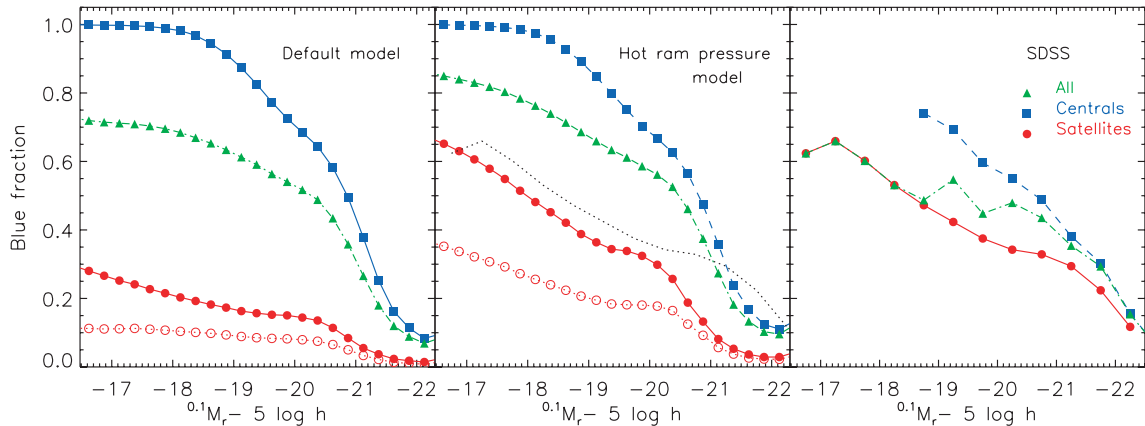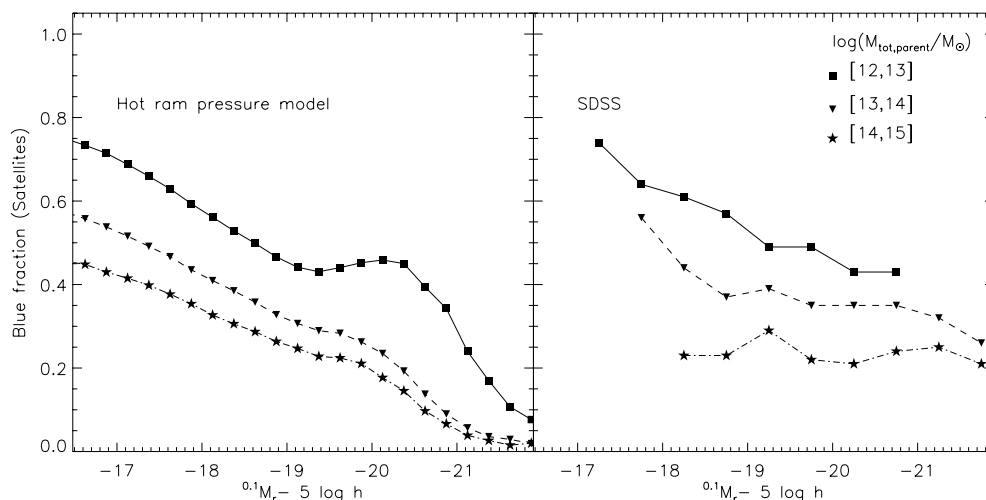

Figure 3. The fraction of blue galaxies per $^{0.1}M_r$ magnitude. The left-hand panel shows the default model, the middle panel shows the hot ram-pressure stripping model. For comparison, we plot in the right-hand panel the fraction of blue galaxies in the SDSS data as derived by Weinmann et al. (2006b). The blue fractions are shown separately for satellites (red circles), central galaxies (blue squares) and all types (green triangles). The empty symbols represent the fraction of blue satellites with the alternative colour cut (see the dashed line in Fig. 2). For better comparison, the black dotted line in the middle panel reproduces the blue fraction of SDSS satellites from the right-hand panel. All magnitudes are k-corrected to redshift 0.1.

As discussed above, the actual fraction of blue galaxies depends on the colour cut adopted; however, the relative difference in the blue fractions between the two models is largely independent of the cut. In particular, we find that using either the Weinmann et al. (2006a) or the alternative cut (or any in between these two), the fraction of satellite galaxies that are blue in the hot ram-pressure model is approximately 2–2.5 times larger than in the default model.

How do the models fare in comparison to the observational data? In the right-hand panel, we show the blue fraction of galaxies mea-

sured by Weinmann et al. (2006b) using an SDSS group catalogue (kindly provided by S. Weinmann). The fraction of satellite galaxies that are blue in the observations increases up to approximately 60 per cent at the faint magnitude end. Encouragingly, the newly implemented ram-pressure model yields a fraction of blue satellites that is in strikingly good agreement with the SDSS results. The satellite blue fraction rises also to about 60 per cent at the faint end and the overall trend in the blue fraction with luminosity is also close to that observed. In contrast, the default model

Figure 4. The fraction of blue satellites per $^{0.1}M_r$ magnitude calculated using the Weinmann et al. colour cut (equation 7), in parent haloes of different mass. The hot ram-pressure stripping model is shown in the left-hand panel. Data from the SDSS group catalogue of Weinmann et al. (2006b) are shown in the right-hand panel. In both panels, magnitudes have been *k*-corrected out to redshift 0.1.

yields a fraction of blue satellite galaxies at most ≈30 per cent (at faint magnitudes). This is similar to the fraction of blue satellites (∼20 per cent) reported for the Croton et al. (2006) semi-analytic model by Weinmann et al. (2006b) (see the bottom right-hand panel of their fig. 4).

We also note that the fraction of bright central galaxies that are blue is in broad agreement with the observations. This is largely a consequence of including a prescription for AGN feedback into GALFORM which tends to halt star formation in the most massive galaxies. Finally, we note that the semi-analytic model predicts many more faint central galaxies than observed in the SDSS group catalogue (independently of how the stripping of the hot-gaseous haloes is treated). However, the lack of faint central galaxies is a selection effect of the group sample in the SDSS: the source catalogue excludes groups for which no member is brighter than $^{0.1}M_r = -19.5 + 5 \log h$, where $h = 0.73$ (Weinmann et al. 2006a). Although we do not attempt to reproduce the mock groups catalogue in detail here, including this selection criterion tends to makes the satellite blue fraction shown in Fig. 3 greater by 0.1, further improving the match to the observations.

3.2 Environmental dependence of colours

ram-pressure stripping is an environmentally driven process, hence one should expect variations in the fraction of blue satellites as a function of parent halo mass. The left-hand panel of Fig. 4 shows the fraction of blue satellites in the hot ram-pressure model per $^{0.1}M_r$ bin, calculated using the Weinmann et al. colour cut (equation 7), for different parent haloes mass ranges. The lower masses, $10^{12} < M_{tot,parent} < 10^{14}$ M$_\odot$, correspond to group-type environments, whereas the larger masses, $M_{tot,parent} > 10^{14}$ M$_\odot$, correspond to massive clusters. For comparison, in the right-hand panel, we plot the blue fractions of satellites in the SDSS group catalogue of Weinmann et al. (2006b) split into the same parent halo mass bins.

Reasonably good agreement with the data is obtained. The new model reproduces the overall trend that satellites of a given magnitude are bluer if they reside in less massive systems. The physical explanation for this behaviour is due to the slightly higher density of the hot gas in more massive systems (because lower mass systems, on average, have converted a larger fraction of their baryons

into stars) and to the higher orbital velocities of satellites in more massive host haloes. The latter effect is the dominant one, especially since the ram-pressure scales with the square of the satellite's velocity. In particular, if we ignore the weak dependence of hot-gas density on halo mass, the ram-pressure scales simply as $P_{ram} \propto v_{sat}^2$. Typically, v_{sat} is of order the virial circular velocity of the parent halo, implying the ram pressure will scale roughly as $P_{ram} \propto M_{tot,p}^{2/3}$. As a result, stripping is more extensive in more massive parent systems, reducing the fuel supply for star formation in satellites.

The model shows a slight increase in the fraction of blue satellite galaxies towards the bright magnitude end, that is the 'bump' at $-19 > {}^{0.1}M_r > -21$. As Fig. 4 shows, this effect is more pronounced for bright galaxies residing in low mass groups, $10^{12} < M_{tot,parent} < 10^{13}$ M$_\odot$, and likely reflects a limitation of the way in which the transition between rapid cooling and hydrostatic regimes is currently treated in the code (see Section 2.1).

The direct comparison between the halo masses in the models and those inferred from the observations should be treated with some caution. In the case of a theoretical model, the true mass of the parent halo is known precisely, however, in the case of the observational data, one must make use of a mass proxy (e.g. Eke et al. 2004). In the particular case of the SDSS data, Weinmann et al. (2006b) use an empirical relationship between the total optical luminosity of a system and its mass. The semi-analytic models, however, show considerable scatter in the relationship between these quantities. Ultimately, one would like to construct a mock survey from the theoretical models with similar characteristics to the SDSS catalogue, and analyse the mock data the same way as the real data. This is beyond the scope of the present paper and will be addressed in a future study.

We also note that similar results have been obtained from studies that attempt to distinguish low mass from high-mass environments using other mass proxies. For example, Hogg et al. (2004) find that bluer galaxies in the local Universe typically reside in low galaxy density environments, whereas redder galaxies tend to live in high galaxy density environments. This is fully consistent with the results of Weinmann et al. (2006b) and our own model predictions if one makes the reasonable assumption that the projected surface density of galaxies increases with increasing parent halo mass (e.g. Gladders et al. 2007).
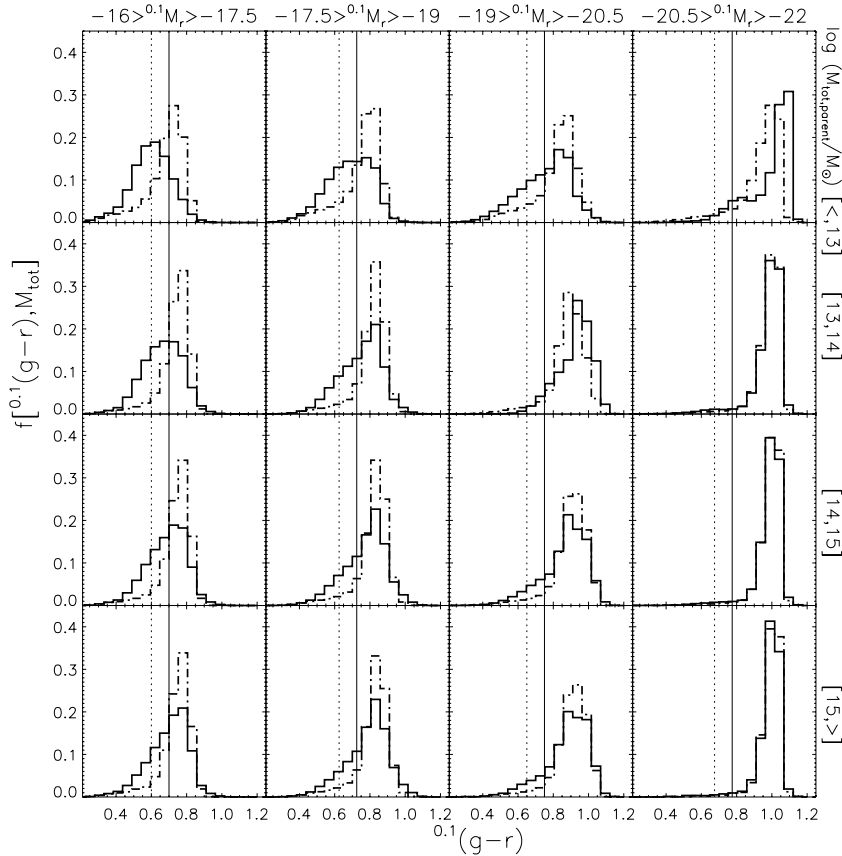
Figure 5. Fraction of satellite galaxies ($f[^{0.1}(g-r), M_{\rm tot}]$) per $^{0.1}(g-r)$ colour bin, divided into different $^{0.1}M_{\rm r}$ magnitude ranges and residing in parent haloes of different total mass. Results for the hot ram-pressure model are plotted with solid lines and for the default model with dot–dashed lines. Magnitudes increase from left- to right-hand side and parent halo mass increase from top towards bottom. Vertical lines correspond to the Weinmann et al. (2006a) colour cut (solid lines) and to the alternative colour cut described in Section 3.1(dotted lines).

Lastly, the colours are expected to depend not only on the mass of the parent halo but also on the intrinsic properties of the satellite. To help disentangle these two factors, we plot in Fig. 5 colour histograms [in $^{0.1}(g-r)$] for satellite galaxies in both the default (dashed lines) and the hot ram-pressure (solid lines) models, divided into different $^{0.1}M_{\rm r}$ magnitude and parent halo mass bins. In the new ram-pressure model, satellites brighter than $^{0.1}M_{\rm r} \sim -20$ tend to be red, independent of the parent halo mass (i.e. environment). This is because internal processes, specifically AGN feedback, are the dominant mechanism for quenching the star formation in these systems. Meanwhile, as expected, low mass satellites in the same model (corresponding to magnitudes fainter than $^{0.1}M_{\rm r} \sim -20$) tend to be bluer in low mass parent haloes and redder in massive clusters. The shapes of the histograms and the overall trends are qualitatively similar to observational results (Balogh et al. 2004; Weinmann et al. 2006a) – but note that the observations include both satellites and centrals. For example, the highest luminosity galaxies are always dominated by the narrow red peak, regardless of environment, a weak tail of blue galaxies only becoming visible in the lowest density regions. Since, we plot only the satellite galaxies here, a distinct blue sequence is not seen; rather, the satellite galaxies increasingly occupy transition colours at low halo masses where star formation has been partially suppressed but not completely extinguished. The results of our model suggest that, at the low halo mass end, environmental processes are as important as the intrinsic physical processes in determining the colour of satellite galaxies.

3.3 Luminosity functions of red and blue galaxies at $z = 0.1$

As a starting point for future comparisons with SDSS and other data, we plot colour luminosity functions for the hot ram-pressure model. Fig. 6 shows the red and blue luminosity functions in the $^{0.1}M_{\rm r}$ band at redshift $z = 0.1$, where colours are separated using the Weinmann et al. cut. Panels include all galaxies (left-hand side), satellites (middle) and central galaxies (right-hand side). Dashed lines represent the default model. Current observational results for the luminosity functions are not able to separate contributions of satellite and central galaxies accurately over this range of luminosity due to the difficulty of robustly identifying faint central galaxies (however, see the recent HOD analysis of Brown et al. 2008). The comparison in Fig. 6 highlights the origin of the variations of the blue fraction seen in Fig. 4.

With the exception of the blue/red luminosity function of satellites, the differences between the default and the hot ram-pressure model are minor. Since, the centrals dominate in total number density, total luminosity functions are similar for both models (cf. discussion of Fig. 1). When all galaxies are combined, the blue galaxy luminosity function has a steeper faint end slope than the red counterpart, in agreement with observational data (e.g. Baldry et al. 2006).[5] By splitting the luminosity function into central and

---

[5] However, a study that appeared after our paper was submitted indicates that the faint end slopes of the red and blue luminosity functions in the
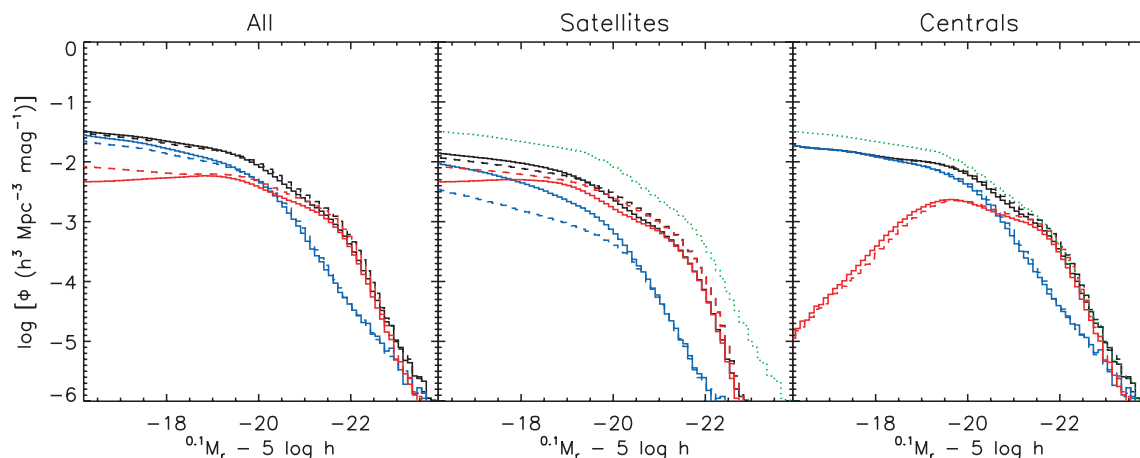
Figure 6. Luminosity functions in the $^{0.1}M_r$ band at redshift $z = 0.1$. Panels include all galaxies (left-hand side), satellites (middle) and central galaxies (right-hand side). Solid lines correspond to the hot ram-pressure model and dashed lines to the default model. Black lines denote all galaxies in the (sub)sample, while red and blue lines denote galaxies that are above and below the $^{0.1}(g - r)$ colour cut in equation (7), respectively. The green dotted lines in the middle and right-hand panels reproduce the total luminosity function of all galaxies for the hot ram-pressure model (solid black line in left-hand panel).

satellite galaxies, we see that this is driven by the rapidly increasing preponderance of blue central galaxies at faint magnitudes. In contrast, the luminosity function of central red galaxies drops by about three orders of magnitude between $^{0.1}M_r$ of -20 and -17. This effect is driven by the AGN feedback in the model, and is independent of the stripping model.

The properties of satellites in the new model are much more dependent on the environmental physics included in the model. In the new model, the blue and red luminosity functions reach similar values at the faint end (consistent with the results in Fig. 3 showing that at the faint end there are roughly similar numbers of red and blue satellites). The dramatic increase in the fraction of faint blue satellites can be seen by comparing the solid and dashed blue lines. This is an alternative way of presenting the information in Fig. 4, and underscores the importance of studying the environmental dependence of galaxy properties in order to obtain a complete picture of galaxy formation and evolution.

4 SUMMARY AND DISCUSSION

Until now, most current semi-analytic models of galaxy formation have adopted a crude modelling of the ram-pressure stripping of the hot-gaseous haloes of satellite galaxies. In particular, they typically assume complete and instantaneous stripping of the hot-gas halo when the galaxy first falls in, without regard for the galaxy's mass, orbit or structural properties. This is at odds with results of hydrodynamic simulations, and also with recent X-ray observations of galaxies in massive clusters. In the present study, we have improved the treatment of stripping by implementing the model of McCarthy et al. (2008) (which has been shown to match simulations of ram-pressure stripping to high accuracy) into the GALFORM semi-analytic model for galaxy formation. Although the initial stripping event does not require us to add additional parameters to the model, subsequent stripping of the gas re-heated from the disc re-

quires additional parameterization. We parametrize this process by assuming that most of the ejecta are retained in the galaxy after the first pericentre passage.

We find that the newly implemented treatment of stripping leads to a significant improvement in the ability of the model to match the colours of satellite galaxies in the SDSS. The new model is also able to account for the environmental dependence of the colours of satellite galaxies. Our results suggest that for the majority of satellite galaxies, this environmental process can be as important in modifying the galaxy colours as intrinsic processes, such as AGN or supernovae feedback, which operate within the satellites themselves. This finding is in broad agreement with previous studies that found that internal processes that quench star formation do not seem capable of explaining the full range of colour and morphology data (e.g. Weinmann et al. 2006a; Baldry et al. 2006).

Although we have only focused on the stripping of hot-gaseous haloes in the present study, other environmental processes may be relevant as well. We now briefly review some of them and conclude that none of them appears to be as important as the ram-pressure stripping of the hot haloes and the feedback already incorporated into our present model.

In cases where the ram-pressure stripping of the hot halo is complete, some stripping of the cold gaseous discs may also occur (Gunn & Gott 1972; Abadi, Moore & Bower 1999; Quilis, Moore & Bower 2000). However, Okamoto & Nagashima (2003) and Lanzoni et al. (2005) have explored ram-pressure stripping of discs in semi-analytic models and have concluded that the effect on the colours and star-formation rates of satellite galaxies are minimal. This most likely stems from the fact that disc stripping is only expected to be relevant for a minority of satellite galaxies whose orbits take them into the very centres of massive systems (e.g. Brüggen & De Lucia 2007).

Thermal evaporation of the hot-gaseous haloes (and/or discs) could also be relevant (Cowie & Songaila 1977), but observational studies of bubbles and cold fronts in X-ray groups and clusters have placed strong constraints on the efficiency of conduction, concluding that it is strongly suppressed (Markevitch & Vikhlinin 2007; McNamara & Nulsen 2007). Turbulent stripping via the generation of Kelvin–Helmholtz and Rayleigh–Taylor instabilities at the interface between the hot-gaseous halo of the satellite and the parent

SDSS DR6 data are shallower than predicted by our model (Montero-Dorta & Prada 2008). If confirmed, this may suggest that other physical processes unaccounted for in our model, e.g. tidal stripping of stars (Henriques et al. 2008), may be responsible for the further flattening of the faint end slopes.

system is possible, but the time-scale for this type of stripping is generally quite long (see McCarthy et al. 2008).

Other possibly relevant processes include viscous stripping (unfortunately at present the viscosity of the hot gas in groups and clusters is poorly constrained; McNamara & Nulsen 2007), tidal effects on the gas as the result of the interaction with the gravitational potential of the parent halo (Byrd & Valtonen 1990; Merritt 1983) or with the other satellites [i.e. mergers (Mihos 1995) or harassment (Moore et al. 1996)], and shock heating of the satellite's hot gas as it falls in at transonic velocities. However, McCarthy et al. (2008) have argued that ram-pressure stripping of the hot-gaseous haloes is always more efficient than tidal stripping by the parent halo's potential or shock heating in cases where the satellite mass is less than about 10 per cent of the parent halo's mass.

In this paper, we have concentrated only on comparisons with data at low redshifts ($z < 0.1$). In a future study, we intend to test the model at other redshifts and compare the redshift evolution of galaxy colours with data from current deep surveys. Another important application of the model is the study of the clustering of galaxies as a function of different physical quantities, such as colour. In addition to the large-scale dependence driven by the relative importance of AGN feedback and ram-pressure stripping as a function of halo mass, our model also predicts a radial dependence within a halo driven by the variation in the strength of stripping with the galaxy orbit. The colour dependence of small-scale clustering will constrain the model and perhaps suggest a way to improve our treatment of the interaction between galaxies and their environment.

Galaxy catalogues for this model are available for download from this http URL: http://galaxy-catalogue.dur.ac.uk:8080/Millennium/

ACKNOWLEDGMENTS

REFERENCES

Abadi M. G., Moore B., Bower R. G., 1999, MNRAS, 308, 947
Baldry I. K., Glazebrook K., Brinkmann J., Ivezić Ž., Lupton R. H., Nichol R. C., Szalay A. S., 2004, ApJ, 600, 681
Baldry I. K., Balogh M. L., Bower R. G., Glazebrook K., Nichol R. C., Bamford S. P., Budavari T., 2006, MNRAS, 373, 469
Balogh M. L., Navarro J. F., Morris S., 2000, ApJ, 540, 113
Balogh M. L., Baldry I. K., Nichol R., Miller C., Bower R., Glazebrook K., 2004, ApJ, 615, 101
Baugh C. M., 2006, Rep. Prog. Phys., 69, 3101
Baugh C. M., Lacey C. G., Frenk C. S., Granato G. L., Silva L., Bressan A., Benson A. J., Cole S., 2005, MNRAS, 356, 1191
Baumgartner W. H., Loewenstein M., Horner D. J., Mushotzky R. F., 2005, ApJ, 620, 680
Bekki K., Couch W. J., 2003, ApJL, 596, L13
Benson A. J., 2005, MNRAS, 358, 551
Benson A. J., Bower R. G., Frenk C. S., Lacey C. G., Baugh C. M., Cole S., 2003, MNRAS, 599, 38
Benson A. J., Lacey C. G., Baugh C. M., Cole S., Frenk C. S., 2002, MNRAS, 333, 156
Binney J., Tremain S., 1987, Galactic Dynamics. Princeton Univ. Press, Princeton, NJ
Blanton M. R. et al., 2003, ApJ, 592, 819
Blanton M. R., Lupton R. H., Schlegel D. J., Strauss M. A., Brinkmann J., Fukugita M., Loveday J., 2005, ApJ, 631, 208
Bower R. G., Benson A. J., Malbon R., Helly J. C., Frenk C. S., Baugh C. M., Cole S., Lacey C. G., 2006, MNRAS, 370, 645 (B06)
Brown M. J. I. et al., ApJ, in press (arXiv:0804.2293)
Bower R. G., McCarthy I. G., Benson A. J., 2008, MNRAS, submitted
Brinchmann J., Charlot S., White S. D. M., Tremonti C., Kauffmann G., Heckman T., Brinkmann J., 2004, MNRAS, 351, 1151
Brüggen M., De Lucia G., 2008, MNRAS, 383, 1336
Byrd G., Valtonen M., 1990, ApJ, 350, 89
Cattaneo A., Dekel A., Devriendt J., Guiderdoni B., Blaizot J., 2006, MNRAS, 370, 1651
Cavaliere A., Fusco-Femiano R., 1976, A&A, 49, 137
Cavaliere A., Fusco-Femiano R., 1978, A&A, 70, 677
Chandrasekhar S., 1943, ApJ, 97, 255
Coil A. L. et al., 2008, ApJ, 672, 153
Cole S., Aragon-Salamanca A., Frenk C. S., Navarro J. F., Zepf S. E., 1994, MNRAS, 271, 781
Cole S., Lacey C. G., Baugh C. M., Frenk C. S., 2000, MNRAS, 319, 168
Cowie L. L., Songaila A., 1977, Nat, 266, 501
Croton D. J. et al., 2006, MNRAS, 365, 11
de Lucia G., Kauffmann G., White S. D. M., 2004, MNRAS, 349, 1101
Eke V. R. et al., 2004, MNRAS, 348, 866
Frei Z., Gunn J. E., 1994, AJ, 108, 1476
Fryxell B. et al., 2000, ApJ, 131, 273
Gladders M. D., Yee H. K. C., Majumdar S., Barrientos L. F., Hoekstra H., Hall P. B., Infante L., 2007, ApJ, 655, 128
Granato G. L., De Zotti G., Silva L., Bressan A., Danese L., 2004, ApJ, 600, 580
Gunn J. E., Gott J. R. III, 1972, ApJ, 176, 1
Harker G., Cole S., Helly J., Frenk C., Jenkins A., 2006, MNRAS, 367, 1039
Helly J. C., Cole S., Frenk C. S., Baugh C. M., Benson A. J., Lacey C., 2003, MNRAS, 338, 903
Henriques B. M., Bertone S., Thomas P., 2008, MNRAS, 383, 1649
Hogg D. W. et al., 2002, AJ, 124, 646
Hogg D. W. et al., 2004, ApJ, 601, 29
Jeltema T. E., Binder B., Mulchaey J. S., 2008, ApJ, 679, 1162
Jones C., Forman W., 1984, ApJ, 276, 38
Kang X., van den Bosch F. C., 2008, ApJ, 676, L101
Kang X., Jing Y. P., Silk J., 2006, ApJ, 648, 820
Kannappan S. J., 2004, ApJ, 611, L89
Kauffmann G., Charlot S., 1998, MNRAS, 294, 705
Kauffmann G., White S. D. M., Guiderdoni B., 1993, MNRAS, 264, 201
Kauffmann G., Colberg J. M., Diaferio A., White S. D. M., 1999, MNRAS, 303, 188
Kauffmann G. et al., 2003, MNRAS, 341, 54
Kauffmann G., White S. D. M., Heckman T. M., Menard B., Brinchmann J., Charlot S., Tremonti C., Brinkman J., 2004, MNRAS, 353, 713
Lacey C., Guiderdoni B., Rocca-Volmerange B., Silk J., 1993, ApJ, 402, 15
Lanzoni B., Guiderdoni B., Mamon G. A., Devriendt J., Hatton S., 2005, MNRAS, 361, 369
Larson R. B., Tinsley B. M., Caldwell C. N., 1980, ApJ, 237, 692
Markevitch M., Vikhlinin A., 2007, Phys. Rep., 443, 1
McCarthy I. G., Frenk C. S., Font A. S., Lacey C., Bower R. G., Mitchell N. L., Balogh M. L., Theuns T., 2008, MNRAS, 383, 593
McNamara B. R., Nulsen P. E. J., 2007, ARA&A, 45, 117
Menci N., Fontana A., Giallongo E., Grazian A., Salimbeni S., 2006, ApJ, 647, 753
Merritt D., 1983, ApJ, 264, 24
Mihos J. C., 1995, ApJ, 438, L75

Montero-Dorta A. D., Prada F., 2008, arXiv e-prints (arXiv:0806.4930v1)

Moore B., Katz N., Lake G., Dressler A., Oemler A., 1996, Nat, 379, 613

Navarro J. F., Frenk C. S., White S. D. M., 1996, ApJ, 462, 563

Navarro J. F., Frenk C. S., White S. D. M., 1997, ApJ, 490, 493

Norberg P. et al., 2002, MNRAS, 336, 907

Nulsen P. E. J., 1982, MNRAS, 198, 1007

Okamoto T., Nagashima M., 2003, ApJ, 587, 500

Quilis V., Moore B., Bower R., 2000, Sci, 288, 1617

Somerville R. S., Primack J. R., 1999, MNRAS, 310, 1087

Springel V., 2005, MNRAS, 364, 1105

Springel V. et al., 2005, Nat, 435, 629

Strateva I. et al., 2001, AJ, 122, 1861

Sun M., Jones C., Forman W., Vikhlinin A., Donahue M., Voit M., 2007, ApJ, 657, 197

Treu T., Ellis R. S., Kneib J.-P., Dressler A., Smail I., Czoske O., Oemler A., Natarajan P., 2003, ApJ, 591, 53

Wang L., Li C., Kauffmann G., De Lucia G., 2007, MNRAS, 377, 1419

Weinmann S. M., van den Bosch F. C., Yang X., Mo H. J., 2006a, MNRAS, 366, 2

Weinmann S. M., van den Bosch F. C., Yang X., Mo H. J., Croton D. J., Moore B., 2006b, 372, 1161

York D. G. et al., 2000, AJ, 120, 1579

This paper has been typeset from a T_EX/L^AT_EX file prepared by the author.